A study of the electrochemical reactivity of titanium under cathodic polarization by means of combined feedback and redox competition modes of scanning electrochemical microscopy

Abdelilah Asserghine[1], Martina Medvidović-Kosanović[3], Livia Nagy[1,2], Ricardo M. Souto[4], Geza Nagy[1,2]

[1]*Department of General and Physical Chemistry, Faculty of Sciences, University of Pécs, 7624, Ifjúság u. 6. Pécs, Hungary*

[2]*János Szentágothai Research Center, University of Pécs, 7624, Ifjúság u. 20. Pécs, Hungary*

[3]*Department of Chemistry, University of Osijek, Cara Hadrijana 8A, HR-31 000 Osijek, Croatia*

[4]*Institute of Materials Science and Nanotechnology, University of La Laguna, P.O. Box 456, E-38200 La Laguna, Tenerife, Canary Islands, Spain*

Abstract

The effect of cathodic polarization on the electrochemical behavior of the thin titanium dioxide film formed by anodic pretreatment over pure commercial titanium metal for biomaterial application was investigated *in situ* using scanning electrochemical microscopy (SECM). Quantitative information on the electron transfer rates (k_{eff}) at the titanium surface was obtained using the feedback operation of SECM using ferrocene-methanol (FcMeOH) as electrochemical mediator. An increase of k_{eff} values with the increase of the negative polarization was detected, a feature that correlates well with the decrease of titanium oxide resistance with increasing cathodic polarization observed using electrochemical impedance spectroscopy (EIS). In addition, SECM operation in the redox competition mode proved that hydrogen was absorbed in the surface oxide film leading to changes in conductivity and electrochemical reactivity.

Keywords

Titanium biomaterial; Thin titanium dioxide layers; Cathodic polarization; Corrosion resistance; SECM; Electron transfer reaction.

1. Introduction

In recent years, titanium and its alloys became very popular biomedical materials due to their biocompatibility, excellent anticorrosion resistance and outstanding mechanical properties such as high strength and low elastic modulus [1-3]. Under atmospheric conditions and in aqueous environments, titanium is spontaneously covered by a passive layer of titanium dioxide with the thickness of a few nanometers [4]. This thin oxide layer exhibits n-type semiconductor property, with band gaps of 3.20 eV for anatase and 3.02 eV for rutile [5], and this accounts for the low electron transfer efficiencies observed in simulated biological conditions [6,7]. But the physicochemical properties of the passivating film are strongly influenced by the composition electrolyte composition [8], particularly by solution pH [9,10], and by electrical polarization [11-13]. The latter feature is of paramount importance with regards to titanium implant devices, because they can become exposed to cathodic polarization due to galvanic coupling with a dissimilar material [14], as it typically happens in hip joint replacements [15,16] and in dental superstructures [17]. For instance, Collier et al. [15] identified localized corrosion of cobalt chromium alloy coupled to Ti6Al4V, which are the major elements of hip joint replacements, whereas Hou and coworkers observed enhanced corrosion rates for magnesium implants coupled to titanium [18]. In addition, cathodic polarization can occur as result of mechanical impact, such as the abrasion induced during the micromotion of the implant with materials such as polymeric cups or another metal [19,20], or even with the adjacent bone [21]. Thus, Contu et al. [22] reported that the mechanical abrasion of c.p. titanium and Ti6Al4V shifted their open circuit potentials (OCP) towards negative values as low as -1.0 V vs. Ag/AgCl. More recently, a similar behavior was observed for binary titanium-niobium and titanium-molybdenum alloys [23].

Metal ion release has been reported for patients bearing prosthetic implants made from titanium and its alloys [24,25], as well as its interaction with serum biomolecules [26]. In addition to wear, polarization of titanium materials affected cell viability during *in vitro* fretting corrosion studies [27]. Furthermore, cytotoxic effects in cell cultures caused specifically by cathodically polarized titanium surfaces have been found for small overvoltages below -0.3 V vs. Ag/AgCl [28-29], a fact leading some authors to suggest that titanium is not the most biocompatible metal [30]. Even more, the high cell killing efficiency achieved by galvanic coupling of titanium with magnesium particles has been proposed as a potential therapy against infection or even cancer [31].

In this work we report a scanning electrochemical microscopy (SECM) investigation of the effect of cathodic polarization on the surface reactivity of the thin oxide layer developed on titanium implantable biomaterial by anodization for the material ensure the passive state of the material. The investigation was performed *in vitro*, that is, while the passivated titanium sample was immersed in a simulated physiological solution at ambient temperature. Although the corrosion resistance of the passive titanium dioxide protective layer is one of the main factors responsible for adequate biocompatibility of titanium-based implants, and numerous studies have focused on investigating the electrochemical behavior of titanium and titanium alloys subjected to different surface treatments and anodic polarizations in different physiological electrolytes [32-37], the electrochemical behavior of cathodically polarized titanium has been scarcely investigated, and the details of the corrosion mechanism are not fully understood yet. SECM has been chosen as the main tool because it has proven very effective for the *in situ* electrochemical characterization of thin oxide films formed on the surface of metals [38,39]. Information on the electrochemical reactivity of the investigated surface can be gathered by operating the SECM in the amperometric feedback mode [40-42], because the SECM tip can collect chemical information from the electrolyte while positioned in close vicinity of the surface of the polarized metal [43].

2. Experimental

Commercial pure titanium metal with 99.99% purity supplied by Goodfellow (Cambridge, UK) with a surface area of 0.016 cm^2 was embedded in *EpoFix* resin sleeve (Struers, Denmark) using a cylindrical mold made of a section of plastic centrifuge tube. A copper wire was connected opposite end of the Ti wire for electric contact. After curing of the resin sleeve, the upper surface of the encased titanium sample was abraded to expose the Ti surface on the planar base. Then it was sequentially wet polished with alumina slurries (diameters of 1, 0.2, and 0.05 µm). The electrochemical cell was built by wrapping cellulose tape around the cylindrical plastic body creating an internal volume of 4 mL. All electrochemical experiments were performed in 0.1 M NaCl solution as testing electrolyte (pH = 6.8) at ambient temperature. Although the experiments were typically performed in the deaerated solution, selected tests were also performed in the naturally aerated electrolyte to ascertain the effect of dissolved oxygen on the electrochemical processes occurring at titanium.

The elemental composition of a freshly polished Ti electrode followed by polarization at +2.0 V vs. Ag/AgCl/ (3 M) KCl for 60 s was made using energy dispersive X-ray

spectroscopy (EDX). The surface preparation was performed in 0.1 M NaCl solution at ambient temperature. An EDX instrument manufactured by Ametek was used to scan an arbitrary area of 220 µm × 165 µm.

Conventional electrochemical tests and electrochemical impedance spectroscopy (EIS) were performed using CHI604E type electrochemical workstation supplied by CH Instruments. The three-electrode configuration was completed using an Ag/AgCl/(3 M) KCl and a platinum wire (diameter 0.5 mm, length 20 mm) as reference and auxiliary electrodes. All potential values in this work are referred to the Ag/AgCl/(3 M) KCl reference electrode. Cyclic voltammetry (CV) measurements were performed on either freshly polished titanium or on titanium samples with a controlled oxide layer formed at +2.00 V for 60 s. In contrast, electrochemical impedance spectroscopy (EIS) was performed on the anodized titanium samples exclusively. Impedance spectra were recorded both on the non-polarized titanium sample (i.e., at the open circuit potential, OCP) and while cathodically polarised between -0.10 and -0.80 V taking 0.10 V increments. The amplitude of the sinusoidal voltage perturbation was 10 mV in the frequency range comprised between 100 kHz and 100 mHz.

The SECM experiments were performed using an Uniscan model 370 (BioLogic, Seyssinet-Pariset, France) combined with a bipotentiostat under computer control. A homemade platinum disk electrode of 25 µm diameter, with RG value of 10, was employed as tip. The small electrochemical cell was completed with Ag/AgCl/(3 M) KCl reference and platinum counter electrodes. Cathodic polarizations were applied to the titanium sample using the second working electrode input of the bipotentiostat.

3. Results and discussion

Preliminary studies were conducted to find the optimum condition for the preparation of a controlled oxide layer on titanium, as well as to identify the redox processes occurring in deaerated 0.1 M NaCl solution at ambient temperature. Firstly, cyclic voltammetry was performed with a freshly polished pure titanium electrode from -0.50 V towards more positive potential, as shown in Figure 1. A fast current increase was immediately observed for potential values more positive than -0.50 V during the first scan in the anodic direction of potential. This potential range with anodic current can be assigned to the formation of a TiO_2 layer on the metal surface according to the reaction [44]:

$$Ti + 2H_2O \rightarrow TiO_2 + 4H^+ + 4e^- \tag{1}$$

Further potential excursion towards more positive values displayed a potential range with stationary current almost up to +2.00 V, thus defining a potential range of stability for the passive oxide film formed on the metal. Upon potential reversal at this switching anodic potential, the current dropped abruptly to values close to zero. Cathodic currents were recorded below -0.10 V, and they steadily grew with further potential excursion towards more negative values although first at a slow pace down to -0.50 V, and then faster for the remaining of the scan. According to Ohtsuka et al. [45], electroreduction of the anodically-formed titanium dioxide layer occurs in this cathodic polarization range. Firstly, electrochemically reduced hydrogen ions get absorbed on the surface according to,

$$H_{aq}^+ + e^- \rightarrow H_{ad} \tag{2}$$
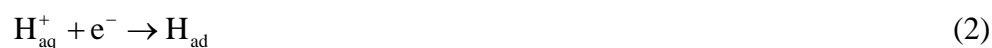
and then, the adsorbed hydrogen contributes to the transformation of titanium dioxide to titanium hydroperoxo species through the reaction [45]:

$$TiO_2 + xH_{aq}^+ + ne^- \rightarrow TiO_{2-x}(OH)_x \tag{3}$$

On the basis of the voltammograms shown in Figure 1, it was decided to apply a potential value of +2.00 V to the titanium samples to form a reproducible oxide layer on their surface. In fact, a reproducible oxide layer on titanium would be required for the investigation of the cathodic polarization effect on the passive film developed anodically over this metal. Figure 2 shows a current-time transient depicting the current flowing from the metal upon application of a potential pulse from the OCP to +2.00 V. The observation of a steady decrease of the current with the elapse of time is consistent with attaining a stable passive current for times longer than 30 s. Therefore, the duration of the passive layer formation stage at this anodic potential was fixed at 60 s for the subsequent work.

The effect of cathodic polarization on the electrochemical reactivity of the titanium sample surface was first investigated using scanning electrochemical microscopy (SECM) in the feedback mode using ferrocene-methanol (FcMeOH) as redox mediator. Titanium samples, with a defined oxide layer formed at +2.00 V for 60 s, were immersed in 0.1 M NaCl + 5 mM FcMeOH solution. The redox mediator was used to enable surface examination while applying different electrical conditions to the titanium sample for differentiation between the

protective characteristics of the oxide layer resulting from the application of cathodic polarization conditions.

When the solution was introduced inside the cell, the tip was positioned over the center of the titanium sample at a vertical (Z) distance of approximately 500 µm. By setting the tip potential at +0.50 V, the diffusion-limited current for ferrocene-methanol oxidation was attained, a value corresponding to the electrochemical response for the tip placed in the bulk of the electrolyte. Next, the tip was moved vertically towards the titanium surface at 1 µm s^{-1} while recording the current measured at the tip as a function of the tip-sample distance. This Z-approach experiment was performed while the titanium sample was left at its open circuit sample potential (OCP), i.e., without applying polarization to the metal. Subsequently, the titanium sample was connected to the potentiostat, and a set of Z-approach curves was recorded for various polarization potentials more negative than the OCP, starting from -0.10 V, and subsequently at increasingly more negative potential values.

The Z-approach curves recorded in the naturally aerated test solution for various polarization conditions are shown as collections of data points in Figure 3A. The abscissa values give the normalized distance L ($L = d/a$, where d is the gap distance between the tip and the titanium sample, and a is the radius of the tip), while the ordinate values show the normalized current $I = I_d/I_\infty$ (where I_d is the tip current measured at the gap distance d, and I_∞ is the current measured in the bulk of the aqueous phase, far from the sample surface). It can be seen that the Z-approach curve recorded at the OCP exhibited a pure negative feedback character because the experimental data closely matched the theoretical line corresponding to an insulator. Since the ferrocene-methanol mediator species could not be recycled on the titanium surface from the ferrocenium ion, it is shown that the oxide layer formed on the sample by anodic polarization was able to effectively passivate the metal surface, thus preventing the occurrence of electron transfer reactions [46]. However, a different situation occurred for the titanium sample polarized at cathodic potential values, and the Z-approach curves gradually deviated from the theoretical approach curve corresponding to an insulating surface as the potential applied to the substrate was made more negative. That is, there was a gradual change in the shape of the Z-approach curves from negative to positive feedback behavior when FcMeOH$^+$ was electroreduced at the cathodically-polarized titanium surface leading to a local increase of the FcMeOH concentration sensed at the SECM tip. Although a predominantly negative feedback behavior could also be observed for the Z-approach curves recorded in the potential range between -0.10 and -0.40 V, a mixed positive-negative feedback behavior was found at the potential of -0.50 V. Furthermore, Z-approach curves

displaying exclusively positive feedback behavior were recorded at potential values more negative than -0.50 V. Subsequently, a new set of Z-approach curves was recorded towards a new titanium sample immersed in deaerated 0.1 M NaCl solution, and they are shown in Figure 3B. It is interesting to notice that the same trends with potential were observed in both cases, thus apparently demonstrating that the effect of cathodic potential towards redox mediator recycling on the surface did not involve the participation of oxygen in this case. Indeed, purely insulating behavior was observed in the sample left unpolarized at its OCP, whereas net transition from negative to positive feedback behavior occurred for titanium polarized at -0.50 V both in the absence and the presence of oxygen in the test electrolyte (cf. Figures 3A and B). Similar shapes and trends were observed for the Z-approach curves with independence of the amount of dissolved oxygen present in the test electrolyte.

Additional confirmation on the electrochemical activation of the titanium surface towards ferrrocene-methanol regeneration as result of cathodic polarization of the metal was achieved using cyclic voltammetry at the platinum tip. The experiments were performed in the deaerated 0.1 M NaCl solution containing 5 mM FcMeOH, that is, the same electrolyte employed to record the Z-approach curves shown in Figure 3B, although in this case the tip was placed over the center of the titanium sample and it was not scanned over the surface. Cyclic voltammograms were then recorded while the titanium surface was polarized at various constant potential values in the range between -0.10 and -0.80 V as to characterize the electrochemical reactivity of the metal under cathodic polarization. Figure 4A shows the cyclic voltammograms recorded while the potential of the platinum tip was scanned between 0 and +0.50 V, i.e. the potential range of ferrocene-methanol oxidation. The characteristic sigmoidal shape of a reversible redox process occurring in a microelectrode was observed in all cases, although the value of the diffusion-limited current greatly depended on the electrical condition of the titanium surface. Thus, the smallest limiting current was determined from the CV measured when the titanium surface was polarized at -0.10 V. In this case the oxide layer on titanium acted as an insulating surface and the electron transfer reaction needed for the reduction of the ferrocenium ion did not occur. Even more, the proximity of the surface to the tip originates a partial hindrance to ferrocene-methanol transport from the bulk electrolyte, thus leading to a smaller limiting current compared to that measured when the tip was located in the bulk of the solution. A progressive increase in the values of the limiting currents was observed by setting the potential at more negative potentials, although its magnitude was not the same with each 100 mV variation. Thus, the change was hardly noticeable for the CV recorded at -0.20 V, and became greater with every potential change down to -0.80 V. Since

the tip-sample distance was not changed during the measurements, the greater availability of ferrocene-methanol for oxidation at the tip could only arise from the recycling of the mediator on the titanium surface as sketched in Figure 4B.

Next, a method of indirectly measuring the corrosion kinetics of the cathodically polarized titanium from the Z-approach curves was performed by using the theoretical models developed by Cornut and Lefrou [47]. In this way, effective rate coefficients (k_{eff}) of the mediator regenerating electrode process were determined [48], a method successfully employed to characterize oxide layers formed on titanium as a function of either the applied anodic potential [13] or the elapsed time [7]. For this purpose, the theoretical Z-approach curves for different values of k_{eff} were calculated by taking in account the geometric parameters of the SECM tip. The best fit between the theoretical and the experimental Z-approach curves was chosen using a least square fitting method, and the resulting curves are shown as lines in Figures 3A and B. It was found that the theoretical curves closely matched the experimental data in all cases. Therefore, the values of k_{eff} obtained in this fitting procedure could be employed to characterize the electrochemical activity of the titanium surface with regards to the conditions applied to the system during the measurement of the individual Z-approach curves, and they are listed in Table 1. It is evident from these results that the insulating characteristics of the oxide layer formed on titanium were progressively lost at increasingly more negative potentials. That is, the variation of the k_{eff} values with the cathodic potential applied to the metal evidenced that electron transfer processes on the oxide-covered surface were progresively facilitated at increasingly more negative potentials, namely varying from ca. 4.0×10^{-4} cm s^{-1} at -0.10 V, to 2.5×10^{-2} cm s^{-1} at -0.70 V. Interestingly, it was found that the values of k_{eff} were practically the same in the deaerated and the naturally aerated solutions for a given cathodic potential value.

The loss of insulating characteristics experienced by the oxide layer anodically-formed on titanium due to the application of a cathodic polarization that was described using local microelectrochemical measurements was further investigated using electrochemical impedance spectroscopy (EIS). First, the impedance spectrum of the oxide-covered titanium surface in 0.1 M NaCl was recorded while the sample was still at its open circuit potential, and the measured impedance data are shown either as Nyquist or Bode diagrams in Figure 5. The characteristic bilayer structure of the oxide films formed on titanium was readily observable from the two time constants occurring in the Bode-phase diagram [49], and it was satisfactorily modelled using the equivalent circuit (EC) shown in Figure 6A. This EC contains the electrolyte resistance R_s in series with two parallel RQ elements, one operating at

higher frequencies that was related to the reactions occurring at the titanium oxide layer/electrolyte interface, namely R_{ct} and Q_{dl}, and another in the low frequency range originating from the resistance and capacitance of the passive oxide layer formed on the metal, R_{ox} and Q_{ox} [50]. Constant phase elements were used instead of pure capacitances due to the distributed relaxation behavior of the surface films. Since capacitance values can be extracted from CPE parameters [51], and after introducing the dielectric constant of TiO_2 ($\varepsilon =$ 65, [52]) following the procedure reported in [53,54], the thickness of the anodically formed titanium oxide layer was determined to be 7 nm, in good agreement with previous reports [55].

Secondly, electrochemical impedance spectra were recorded applying different constant polarization potential values to the titanium sample from -0.10 down to -0.80 V. Figure 5A shows the Nyquist plots measured for the polarized metal in addition to that obtained at the OCP, revealing depressed semi-semicircles of varying size. Their radius decreased with the increase of the cathodic polarization applied to the sample. Since the corresponding Bode diagrams depicted in Figure 5B revealed the occurrence of two time constants in this case as well, the impedance spectra were modeled using the EC of Figure 6A, and the corresponding resistance and capacitance values of the oxide layer were plotted as a function of the applied potential in Figure 6B. Although the values of R_{ox} showed a small variation with the potential up to -0.30 V, a clear decrease of the resistance occurred for polarizations more negative than -0.40 V. This trend for R_{ox} was accompanied by an increase of the capacitance of the oxide layer, C_{ox}, that can be attributed to a progressive thinning of the passive film. Very importantly, the effect of the cathodic polarization on the impedance parameters corresponding to the oxide film was observed to occur in a similar way to the potential dependence of the k_{eff} values derived from the SECM data given in Figure 3 (cf. Table 1).

Further insights into the effect of cathodic polarization to produce changes in the electrochemical activity of the oxide layer formed on titanium was obtained by recording 2D SECM maps over the complete titanium surface immersed in deaerated 0.1 M NaCl + 5 mM FcMeOH solution. The potential of the 25 μm dia. measuring SECM tip was maintained at +0.50 V, and it was scanned with a scan rate of 20 μm s^{-1} over the sample at constant tip-sample distance of 20 μm. The first SECM map was recorded for the sample at its OCP, followed by a sequence of 2D images recorded at fixed cathodic polarization potentials progressively set increasingly more negative values. The recorded SECM images are presented as normalized current (I_d/I_∞), given in Figure 7. The map recorded at the OCP

shows an almost homogeneous current distribution around the normalized value of 0.63 over the complete scanned area. It is evident that the current values recorded over the oxide-covered metal and above the epoxy sleeve were the same, and the contour of the metal could not be distinguished from the surrounding resin in the image (see the map in Figure 7A, where the contour of the metal was drawn to help recognizing its actual position in the SECM map). All the exposed area acted as an insulator with negative feedback response, and recycling of the redox mediator did not occur in the system. This feature agrees with the occurrence of a negative-feedback shape in the Z-approach curve determined at the OCP of the oxide-covered titanium samples in both the deaerated and the naturally-aerated solutions (see the black colored data points in Figures 3A and B).

Higher tip currents were recorded when the titanium sample was biased to cathodic potentials with respect to the OCP, always resulting in the measurement of higher values over the titanium surface than above the insulating resin. In this way, normalized current values of 0.92, 1.08 and 1.35 where observed above the sample for applied substrate potentials of -0.40, -0.60 and -0.80 V, respectively (cf. Figure 7B-D). This behaviour resulted from electron transfer donation from the oxide-covered titanium to the dissolved ferrocenium species confined in the small electrolyte volume comprised between the tip and the substrate, and it results in a positive feedback effect as proven by the corresponding Z-approach curves depicted in Figure 3. In addition, it must be noticed that rather uniform current distributions were observed in the 2D-SECM maps regardless depicting negative or positive feedback effects for titanium when they were measured at its OCP or under cathodic polarization, respectively. This fact evidences the homogeneity of the oxide-coated titanium surface produced by anodic polarization at +2.00 V, as well as the high purity of the titanium sample.

This is in good agreement with the homogeneous chemical distributions of oxygen and titanium evidenced by energy dispersive X-ray spectroscopy. Figure 8 shows a typical spectrum and the corresponding oxygen and titanium distributions found on the titanium surface. As it can be seen, only oxygen and titanium are detected at the surface of the retrieved sample. In addition, these two elements are found to be homogeneously distributed over the surface of the material. Since the estimated weight percentages of oxygen and titanium are 27.5% and 72.5%, respectively, thus corresponding to an almost 1:1 atomic ratio. Therefore, some contribution of the underlying titanium metal to the recorded signal must be considered, thus supporting our suggestion of a thin oxide layer formed on the metal of the surface. This feature agrees well with the estimated thickness of 7 nm for the oxide layer that was determined from EIS data.

In summary, the electrochemical behavior derived from the analysis of the 2D SECM images and the *Z*-approach curves recorded in these experiments supports that the negative polarization potential increases the conductivity of the titanium oxide layer on the metal.

So far, the positive feedback response observed in the *Z*-approach curve experiments and SECM images under cathodic polarization seen was explained by considering the surface film evolving from a passive to a more conductive oxide condition. But the shape of the cyclic voltammograms of the titanium sample shown in Figure 1 in the negative potential range could be explained in terms of the electrochemical reduction of titanium dioxide (according to equation (2)) accompanied by the absorption of hydrogen. That is, when a more cathodic polarization potential was applied, more hydrogen could be absorbed in the oxide film [45]. Since titanium dioxide exhibits a semi-conductive property [56], the mentioned processes would result in the availability of additional electronic states within the band gap of titanium oxide [57]. This feature would increase its conductivity as a function of the applied substrate potential [57,58], reaching a limiting conductivity around -0.80 V (cf. Figure 6B). Hence, the assumptions of increased surface conductivity and facilitated electron transfer at the titanium oxide film can be supported.

Since the titanium sample was polarized negatively, the eventual evolution of hydrogen from the surface should be taken in account, because its oxidation at the platinum tip would contribute to the measured current, thus effectively interfering with the oxidation of FcMeOH as described above. To clarify this point, cyclic voltammetry at the platinum tip was performed to characterize the redox processes occurring in the deaerated 0.1 M NaCl solution in the absence of the redox mediator (FcMeOH). In the experiments, the platinum tip was maintained at a fix location approximately above the center of the titanium sample, with a tip-sample distance of 10 μm, and it was not scanned over the surface. The cyclic voltammograms were recorded at the tip while the titanium surface was polarized at various constant potential values in the range between -0.10 and -0.80 V as to characterize the electrochemical activity of the metal under cathodic polarization conditions, and they are shown in Figure 9. The occurrence of an oxidation current was monitored at the tip for potentials more positive than 0.0 V, leading to the development of a current plateau extending from +0.20 to +0.50 V, that is, within the potential range for ferrocene-methanol oxidation in Figure 4A. Nevertheless, it must be noticed that the current scales used in Figures 4A and 9 differ by two orders of magnitude, thus effectively showing that eventual hydrogen evolution resulting from the cathodic polarization of the titanium surface down to -0.80 V would not contribute appreciably interfere the observations derived from the SECM experiments

performed adding 5 mM FcMeOH to the test electrolyte. An additional confirmation was gathered using the SECM in the sample generation-tip collection mode (SG/TC) as sketched in Figure 109A. In these experiments the platinum tip was polarized at 0 V whereas the oxide-coated titanium sample was biased at different cathodic polarization values in the potential range from -0.10 to -1.40 V. First, the platinum tip was positioned at 20 μm from the surface by recording a Z-approach curve above the insulating resin in 0.1 M NaCl + 5 mM FcMeOH solution. Accordingly, a negative feedback behaviour was observed, and the tip position was determined by fitting the measured approach curve to the theoretical one. Then the tip was positioned for 20 μm vertical distance from the sample surface. Subsequently, the solution was replaced by deareated 0.1 M NaCl solution, prior to recording a series of SECM line scans by shifting the tip parallel to the metal surface with a scan rate of 10 μm s^{-1}. The set of SECM line scans recorded for different potential values applied to the sample are shown in Figure 10B. The sequence of measurement was initiated at the most positive potential in the interval, and progressively applying a more negative polarization to the sample. As it can be observed from the inspection of Figure 10B, stationary current plots close to 0 nA were recorded above titanium sample when the applied polarizing potentials were set between -0.10 and -1.20 V. This fact evidenced that no detectable hydrogen gas evolution occurred on the surface for these cathodic polarizations. It implies that the reduction (thinning) of the oxide film on the metal is the dominant electrochemical process taking place in the potential range down to -1.20 V, in agreement with the findings reported by Zeng et al. [59]. Conversely, a significant current was recorded at the tip when it passed over the metal sample with an applied potential of -1.40 V, thus proving the evolution of hydrogen gas from the titanium surface at this negative polarization. In addition, the line scan showed higher concentrations of evolved hydrogen close to the edges of the titanium sample. Altogether, the experiments shown in Figures 9 and 10 prove that no measurable hydrogen gas evolution happened as result of cathodic polarization in the investigated potential range down to -0.80 V, and the tip currents measured during the feedback experiments depicted in Figure 4 resulted only from the oxidation of FcMeOH at the probe.

Further insight into the effect of cathodic polarization on the electrochemical activation of oxide coated titanium was attained using SECM by setting the tip potential to -0.60 V in order to monitor the concentration of the hydrogen ion present in the confined electrolyte volume between the tip and the metal sample [60]. In this case, the electrochemical process producing a current signal at the tip arises from the reduction of the hydrogen ion as sketched in Figure 11A. In the new set of experiments, 6000 μm long horizontal line scans

were recorded over the center of an oxide coated titanium sample embedded in epoxy resin, that was immersed in deaerated 0.1 M NaCl test solution. The vertical distance between the SECM probe and the sample surface was set to 20 µm using the same procedure previously described for the recording of the scan line depicted in Figure 10B. Figure 11B shows selected plots obtained at various substrate polarizations. They are effectively current–distance data recorded as the tip travelled parallel to the titanium sample 20 µm above it. As it can be seen, stationary current plateaus for hydrogen ion reduction were recorded above the insulating resin regardless the polarization applied to the sample, this effect being better observed at the left of the plots, whereas at the right side convective effects due to the movement of the tip accounted for the less abrupt change between the metal and the resin. Conversely, the current values measured over the metal greatly varied on the applied polarizing potential. In this way smaller tip currents were recorded for increasingly more negative potentials applied to the substrate. This feature can be explained by the onset of a competitive effect in the SECM system. That is, when a sufficiently cathodic polarization potential is applied on the titanium surface such as the reduction reaction of hydrogen ions can occur on the titanium surface according to equation (2), the substrate would effectively compete with the tip for this species. As result, the concentration of hydrogen ions would decrease in the vicinity of titanium, and less species would be available for the reduction reaction at the tip resulting in a measurable decrease of the tip current as the tip scans the metal. This is the so-called redox-competition mode of the SECM [**¡Error! Marcador no definido.**,**¡Error! Marcador no definido.**] and it is illustrated in Figure 11A as well. As readily seen, the precise location of the titanium sample was hardly distinguishable from the surrounding resin when the line scan was recorded above the sample polarized at -0.30 V, an evidence that the oxide coated metal did not significantly contribute to the electroreduction of hydrogen ions from the nearby electrolyte at this cathodic polarization. A small competitive effect showed up when the applied potential was -0.40 V, showing that the rate of electrochemical reduction is slow in the vicinity of titanium. For substrate potential values more negative than -0.50 V, an intense competitive effect could be observed owing to the significant decrease of hydrogen ion reduction at the tip, leading to a 5-fold decrease of the tip currents recorded over the metal when the tip scans at 20 µm distance from the metal. This finding is in good agreement with the voltammograms depicted in Figure 1 that showed an increase of the reduction current when the potential excursion at the titanium sample was more negative than -0.50 V. Indeed, it has been reported that hydrogen is significantly absorbed on the surface of titanium according to equation (2) in this potential range [45]. In

correlation with these findings, the *Z*-approach curve experiments given in Figure 3 showed that the oxide-covered titanium became more conductive at potentials below -0.50 V, whereas a considerable decrease of the resistance of the oxide layer on titanium was measured by EIS (cf. Figure 6B). Unfortunately, the results described here are not in accordance with the findings reported by Gilbert et al. [28] by operating the SECM in the redox-competition mode for the monitoring of oxygen reduction on titanium metal. In their experiments, the metal was biased to negative potentials in the range between -0.10 and -1.00 V using 0.10 V steps. They noticed that the tip current decreased with increasing negative polarization, and no measurable tip currents occurred for polarizations of -0.90 V and beyond. In that work, the interpretation of the experimental findings regarding the electrochemical activity of the titanium sample was based on considering that the current measured at the SECM tip resulted from oxygen reduction, but this assumption may not be correct. On the basis of the experiments described here, the tip current measurements by Gilbert et al. [28] most likely arose from the amperometric reduction of hydrogen ions, whereas dissolved oxygen did not participate in the electrode process. Indeed, there are reports in the literature proving that oxygen reduction on titanium only occurs at potentials more negative than -1.00 V in neutral and alkaline environments [61,62]. This feature may account for the decreased viability of the cells of the surrounding tissue in the case of titanium implants *in vivo* [27,28,31].

4. Conclusion

A combination of operation modes in amperometric SECM has shown to be a powerful tool for the investigation of the effect of cathodic polarization on a previously anodized titanium material, thus matching the usual surface condition of the material used for implantology. In this way, more detailed information on the process could be gained than using conventional electrochemical techniques such as cyclic voltammetry and electrochemical impedance (EIS), although the results of these surface-averaging techniques supported the conclusions obtained on the basis of SECM data.

It was demonstrated that the conductive property of the thin titanium dioxide layer formed on commercial pure titanium metal surface can change upon cathodic polarization. The passive protective film can acquire a more conductive oxide structure when it is polarized at sufficiently cathodic potentials during immersion in an aqueous electrolyte even under deaerated conditions. The reported conductivity changes of the surface film were evidenced using the feedback mode of SECM, and could be quantitatively described in terms of electron

transfer rates (k_{eff}) at the titanium surface. The potential dependence of k_{eff} values satisfactorily matched the observed variation of the resistance and capacitance of the oxide film observed using EIS.

Using the generation-collection mode of SECM, it was demonstrated that evolution of hydrogen gas from the cathodically-polarized titanium surface did not occur at small and moderate polarizations down to -0.80 V vs. Ag/AgCl/(3 M) KCl. Nevertheless, hydrogen ion reduction is the main reduction process accompanying thinning of the oxide film, leading to the absorption of atomic hydrogen by the metal substrate. The occurrence of this reaction was demonstrated using a redox competition mode of SECM. As result, it is proposed that the cathodic polarization produces a decrease of titanium oxide resistance (as demonstrated by EIS), the increase of the electron transfer on the oxide film as shown by SECM in the feedback mode, as well as hydrogen intercalation into the titanium dioxide film proved by monitoring the hydrogen ion concentration in the adjacent electrolyte by SECM in the redox-competition mode.

These results described in this work show that the high anticorrosion characteristics of an oxide-coated titanium biomaterial are severely harmed under cathodic polarization conditions, as evidenced by the considerable change of electrical conductivity and the occurrence of electron transfer reactions at the titanium oxide/electrolyte interface. This may result in the occurrence of faster corrosion rates for titanium in the physiological environment, as well as accounting for a decrease in cell viability in the surrounding tissues.

References

1. M. Geetha, A.K. Singh, R. Asokamani, A.K. Logia, Ti based biomaterials, the ultimate choice for orthopaedic implants – a review, Progress in Materials Science 54 (2009) 397-425.

2. C. Veiga, J.P. Davim, A.J.R. Loureiro, Properties and applications of titanium alloys: a brief review, Reviews on Advanced Materials Science 32(2012) 14-34.

3. F.H. Froes, Titanium for medical and dental applications—An introduction, in: Titanium in Medical and Dental Applications, F.H. Froes, M. Qian (Eds.), Woodhead Publishing, Duxford, United Kingdom, 2018, pp. 3-21. https://doi.org/10.1016/B978-0-12-812456-7.00001-9

4. B.G. Pound, Passive films on metallic biomaterials under simulated physiological conditions, Journal of Biomedical Materials Research Part A 102 (2014) 1595-1604.

5. M.V. Diamanti, S. Codeluppi, A. Cordioli, M.P. Pedeferri, Effect of thermal oxidation on titanium oxides' characteristics, Journal of Experimental Nanoscience 4 (2009) 365-372.

6. S.E. Pust, D. Scharnweber, S. Baunack, G. Wittstock, Electron transfer kinetics at oxide films on metallic biomaterials Scanning electrochemical microscopy studies of Ti6Al4V, Journal of The Electrochemical Society 154 (2007) C508-C514.

7. A. Asserghine, D. Filotás, L. Nagy, G. Nagy, Scanning electrochemical microscopy investigation of the rate of formation of a passivating TiO_2 layer on a Ti G4 dental implant, Electrochemistry Communications 83 (2017) 33-35.

8. X. Cheng, S.G. Roscoe, Corrosion behavior of titanium in the presence of calcium phosphate and serum proteins, Biomaterials 26 (2005) 7350-7356.

9. M.E.P. Souza, L. Lima, C.R.P. Lima, C.A.C. Zavaglia, C.M.A. Freire, Effects of pH on the electrochemical behavior of titanium alloys for implant applications, Journal of Materials Science: Materials in Medicine 20 (2009) 549-552.

10. E. Brooks, M. Tobias, K. Krautsak, M. Ehrensberger, The influence of cathodic polarization and simulated inflammation on titanium electrochemistry, Journal of Biomedical Materials Research Part B: Applied Biomaterials 102 (2010) 1445-1553.

11. M.T. Ehrensberger, J.L. Gilbert, The effect of static applied potential on the 24-hour impedance behavior of commercially pure titanium in simulated biological conditions, Journal of Biomedical Materials Research Part B: Applied Biomaterials 93 (2010) 106-112.

12. Z.Bai, H.H. Rotermund, The intrinsically high pitting corrosion resistance of mechanically polished nitinol in simulated physiological solutions, Journal of Biomedical Materials Research Part B: Applied Biomaterials 99 (2011) 1-13.

13. J. Izquierdo, M.B. González-Marrero, M. Bozorg, B.M. Fernández-Pérez, H.C. Vasconcelos, J.J. Santana, R.M. Souto, Multiscale electrochemical analysis of the corrosion of titanium and nitinol for implant applications, Electrochimica Acta 203 (2016) 366-378.

14. N. Eliaz, Corrosion of metallic biomaterials: A review, Materials 12 (2019) 407, 91 pp. https://doi.org/10.3390/ma12030407.

15. J.P. Collier, V.A. Suprenant, R.E. Jensen, M.B. Mayor, Corrosion at the interface of cobalt alloy heads on titanium-alloy items, Clinical Orthopaedics and Related Research 271 (1991) 305-311.

16. H.S. Hothi, A.C. Panagiotopoulos, R.K. Whittaker, P.J. Bills, R.A. McMillan, J.A. Skinner, A.J. Hart, Damage patterns at the head-stem taper junction helps understand the mechanisms of material loss, The Journal of Arthroplasty 32 (2017) 291-295.

17. A. Mellado-Valero. A.I. Muñoz, V.G. Pina, M.F. Sola-Ruiz, Electrochemical behaviour and galvanic effects of titanium implants coupled to metallic suprastructures in artificial saliva, Materials 11 (2018) 171, 19 pp. https://doi.org/10.3390/ma11010171.

18. P. Hou, P. Han, C.L. Zhao, H.L. Wu, J.H. Ni, S.X. Zhang, J.Y. Liu, Y.Z. Zhang, H.D. Xu, P.F. Cheng, S. Liu, Y.F. Zheng, X.N. Zhang, Y.M. Chai, Accelerating corrosion of pure magnesium co-implanted with titanium in vivo, Scientific Reports 7 (2017) 41924, 10 pp. https://doi.org/10.1038/srep41924.

19. D.W. Hoeppner, V. Chandrasekaran, Fretting in orthopaedic implants: a review, Wear 173 (1994) 189-197.

20. J. Geringer, B. Forest, P. Combrade, Fretting-corrosion of materials used as orthopaedic implants, Wear 259 (2005) 943-951.

21. J. Geringer. B. Boyer, K. Kim, Fretting corrosion in biomedical implants, In: Tribocorrosion of Passive Metals and Coatings, D. Landolt, S. Mischler (Eds.), Woodhead Publishing, Cambridge, UK, 2011, pp. 401-423.

22. F. Contu, B. Elsener, H. Ovni, A study of the potentials achieved during mechanical abrasion and the repassivation rate of titanium and Ti6Al4V in inorganic buffer solutions and bovine serum, Electrochimica Acta 50 (2004) 33-41.

23. J. Ureña, S. Tsipas, A. M. Pinto, F. Toptan, E. Gordo, A. Jiménez-Morales, Corrosion and tribocorrosion behaviour of β-type Ti-Nb and Ti-Mo surfaces designed by diffusion treatments for biomedical applications, Corrosion Science 140 (2018) 51-60.

24. S. Ichinose, T. Muneta, I. Sekiya, S. Itoh, H. Aoki, M. Tagami, The study of metal ion release and cytotoxicity in Co–Cr–Mo and Ti–Al–V alloy in total knee prosthesis, Journal of Materials Science: Materials in Medicine 14 (2003) 79-86.

25. A. Sarmiento-González, J.M. Marchante-Gayón, J.M. Tejerina-Lobo, J. Paz-Jiménez, A. Sanz-Medel, High resolution ICP-MS determination of Ti, V, Cr, Co, Ni, and Mo in

human blood and urine of patients implanted with a hip or knee prosthesis, Analytical and Bioanalytical Chemistry 391 (2008) 2583-2589.

26. Y. Nuevo-Ordónez, M. Montes-Bayón, E. Blanco-González, J. Paz-Aparicio, J.D. Raimundez, J.M. Tejerina, M.A. Pena, A. Sanz-Medel, Titanium release in serum of patients with different bone fixation implants and its interaction with serum biomolecules at physiological levels, Analytical and Bioanalytical Chemistry 401 (2011) 2747-2754.

27. T. Hui, G.W. Kubacki, J.L. Gilbert, Voltage and wear debris from Ti-6Al-4V interact to affect cell viability during in-vitro fretting corrosion, Journal of Biomedical Materials Research Part B: Applied Biomaterials 106 (2018) 160-167.

28. J.L. Gilbert, L. Zarka, E. Chang, C.H. Thomas, The reduction half-cell in biomaterials corrosion: Oxygen diffusion profiles near and cell response to polarized titanium surfaces, Journal of Biomedical Materials Research 42(1998) 321-330.

29. S. Sivan, S. Kaul, J.L. Gilbert, The effect of cathodic electrochemical potential of Ti-6Al-4V on cell viability: Voltage threshold and time dependence, Journal of Biomedical Materials Research Part B: Applied Biomaterials 101 (2013) 1489-1497.

30. M. T. Ehrensberger, S. Sivan, J.L. Gilbert, Titanium is not "the most biocompatible metal" under cathodic potential: The relationship between voltage and MC3T3 preosteoblast behavior on electrically polarized cpTi surfaces, Journal of Biomedical Materials Research Part A 93 (2010) 1500-1509.

31. J. Kim, J.L. Gilbert, Cytotoxic effect of galvanically coupled magnesium-titanium particles, Acta Biomaterialia 30 (2016) 368-377.

32. G.T. Burstein, R.M. Souto, Observations of localized instability of passive titanium in chloride solution, Electrochimica Acta 40 (1995) 1881-1888.

33. C.E.B. Marino, E.M. Oliveira, R.C. Rocha-Filho, S.R. Biaggio, On the stability of thin-anodic-oxide films of titanium in acid phosphoric media, Corrosion Science 43 (2001) 1465-1476.

34. G.T. Burstein, C. Liu, R.M. Souto, The effect of temperature on the nucleation of corrosion pits on titanium in Ringer's physiological solution, Biomaterials 26 (2005) 245-256.

35. V.A. Alves, R.Q. Reis, I.C.B. Santos, D.G. Souza, T. de F. Goncalves, M.A. Pereira-da-Silva, A. Rossi, L.A. da Silva, In situ impedance spectroscopy study of the electrochemical corrosion of Ti and Ti-6Al-4V in simulated body fluid at 25°C and 37°C, Corrosion Science 51 (2009) 2473-2482.

36. A. Mazzarolo, M. Curioni, A. Vicenzo, P. Skeldon, G.E. Thompson, Anodic growth of titanium oxide: electrochemical behaviour and morphological evolution, Electrochimica Acta 75 (2012) 288-295.

37. G. Wang, Y. Wan, T. Wang, Z. Liu, Corrosion behavior of titanium implant with different surface morphologies, Procedia Manufacturing 10 (2017) 363-370.

38. D.E. Tallman, M.B. Jensen, Applications of scanning electrochemical microscopy in corrosion research, in: Scanning Electrochemical Microscopy, Second Edition, A.J. Bard, M.V. Mirkin (Eds.), CRC Press, Boca Raton, FL, 2012, pp. 451-488.

39. N.A. Payne, L.I. Stephens, J. Mauzeroll, The application of Scanning Electrochemical Microscopy to corrosion research, Corrosion 73 (2017) 759-780.

40. B. Csóka, B. Kovács, G. Nagy, Investigation of concentration profiles inside operating biocatalytic sensors with scanning electrochemical microscopy (SECM), Biosensors and Bioelectronics 18 (2003) 141-149.

41. S.E. Pust, D. Scharnweber, C.N. Kirchner, G. Wittstock, Heterogeneous distribution of reactivity on metallic biomaterials: scanning probe microscopy studies of the biphasic Ti alloy Ti6Al4V, Advanced Materials 19 (2007) 878-882.

42. R. Zhu, Z. Qin, J.J. Noël, D. W. Shoesmith, Z. Ding, Analyzing the influence of alloying elements and impurities on the localized reactivity of titanium grade-7 by scanning electrochemical microscopy, Analytical Chemistry 80 (2008) 1437-1447.

43. D. Polcari, P. Dauphin-Ducharme, J. Mauzeroll, Scanning electrochemical microscopy: a comprehensive review of experimental parameters from 1989 to 2015, Chemical Reviews 116 (2016) 13234-13278.

44. R.M. Torresi, O.R. Cámara, C.P. De Pauli, Influence of the hydrogen evolution reaction on the anodic titanium oxide film properties, Electrochimica Acta 32 (1987) 1357-1363.

45. T. Ohtsuka, M. Masuda, N. Sato, Cathodic reduction of anodic oxide films formed on titanium, Journal of The Electrochemical Society 134 (1987) 2406-2410.

46. A.J. Bard, Introduction and principles, in: Scanning Electrochemical Microscopy, Second Edition, A.J. Bard, M.V. Mirkin (Eds.), CRC Press, Boca Raton, FL, 2012, pp. 1-14.

47. R. Cornut, C. Lefrou, New analytical approximation of feedback approach curves with a microdisk SECM tip and irreversible kinetic reaction at the substrate, Journal of Electroanalytical Chemistry 621 (2008) 178-184.

48. S.E. Pust, W. Maier, G. Wittstock, Investigation of localized catalytic and electrocatalytic process and corrosion reactions with scanning electrochemical microscopy (SECM), Zeitschrift für Physikalische Chemie 222 (2008) 1463-1517.

49. J. Pan, D. Thierry, C. Leygraf, Electrochemical impedance spectroscopy study of the passive oxide film on titanium for implant application, Electrochimica Acta 41 (1996) 1143-1153.

50. F. Mansfeld, Analysis and Interpretation of EIS Data for Metals and Alloys, Technical Report 26, Solartron-Schlumberger, Hampshire, 1993, Ch. 4.

51. J.R. Macdonald, Note on the parametrization of the constant-phase adimittance element, Solid State Ionics 13 (1984) 147-149.

52. J. Pan, D. Thierry, C. Leygraf, Electrochemical and XPS studies of titanium for biomaterial applications with respect to the effect of hydrogen peroxide, Journal of Biomedical Materials Research 28 (1994) 113-122.

53. B. Hirschorn, M.E. Orazem, B. Tribollet, V. Vivier, I. Frateur, M. Musiani, Determination of effective capacitance and film thickness from constant-phase-element parameters, Electrochimica Acta 55 (2010) 6218-2227.

54. G. Bolat, J. Izquierdo, J.J. Santana, D. Mareci, R.M. Souto, Electrochemical characterization of ZrTi alloys for biomedical applications, Electrochimica Acta 88 (2013) 447-456.

55. T. Hurlen, S. Hornjkol, Anodic growth of passive films on titanium, Electrochimica Acta 36 (1991) 189-195.

56. X. Chen, S.S. Mao, Titanium dioxide nanomaterials: Synthesis, properties, modifications, and applications, Chemical Reviews 107 (2007) 2891-2959.

57. J.M. Macak, H. Tsuchiya, A. Ghicov, K. Yasuda, R. Hahn, S. Bauer, P. Schmuki, TiO_2 nanotubes: Self-organized electrochemical formation, properties and applications, Current Opinion in Solid State Materials Science 11 (2007) 3-18.

58. A. Fujishima, X.T. Zhang, D.A. Tryk, TiO_2 photocatalysis and related surface phenomena, Surface Science Reports 63 (2008) 515-582.

59. Y. Zeng, J.J. Noël, P.R. Norton, D.W. Shoesmith, Hydrogen transport through thin titanium oxides, Journal of Electroanalytical Chemistry 649 (2010) 277-285.

60. J. Zhou, Y. Zu, A.J. Bard, Scanning electrochemical microscopy Part 39. The proton/hydrogen mediator system and its application to the study of the electrocatalysis of hydrogen oxidation, Journal of Electroanalytical Chemistry 491 (2000) 22-29.

61. S.V. Mentus, Oxygen reduction on anodically formed titanium dioxide, Electrochimica Acta 50 (2004) 27-32.

62. V.B. Baez, J.E. Graves, D. Pletcher, The reduction of oxygen on titanium oxide electrodes, Journal of Electroanalytical Chemistry 340 (1992) 273-286.

Table 1. Effect of the applied cathodic potential on the kinetic rate constants for FcMeOH$^+$ electroreduction on oxide-covered titanium samples during immersion in either deaerated or naturally aerated 0.1 M NaCl test solutions. The kinetic rate constants were calculated from the Z-approach curves depicted in Figure 3.

In deaerated 0.1 M NaCl		In naturally aerated 0.1 M NaCl	
Potential, V vs. Ag/AgCl/(3 M) KCl	k_{eff} **, cm s^{-1}**	**Potential, V vs. Ag/AgCl/(3 M) KCl**	k_{eff} **, cm s^{-1}**
-0.70	0.0250	-0.70	0.0100
-0.60	0.0050	-0.65	0.0060
-0.50	0.0019	-0.60	0.0050
-0.40	0.0010	-0.55	0.0035
-0.3	0.00065	-0.40	0.0016
-0.2	0.00050	-0.35	0.0012
-0.1	0.00040	-0.20	0.00075
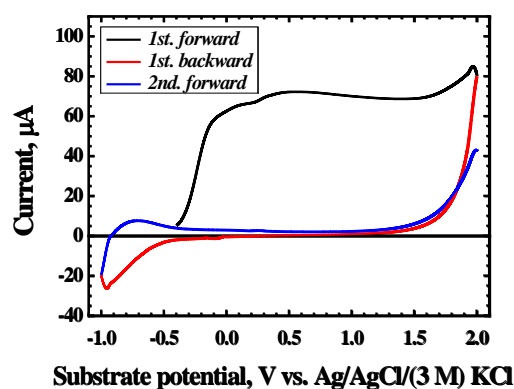
Figure 1. Cyclic voltammetry of a freshly polished titanium sample immersed in deaerated 0.1 M NaCl solution. Scan rate: 50 mV s^{-1}.
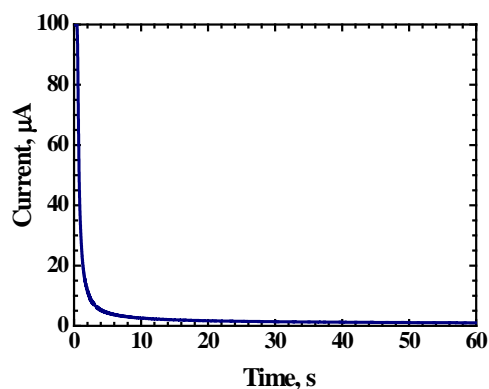
Figure 2. Current transient recorded on a freshly polished titanium immersed in deaerated 0.1 M NaCl solution upon the application of a potentiostatic pulse at +2.00 V vs. Ag/AgCl/(3 M) KCl.
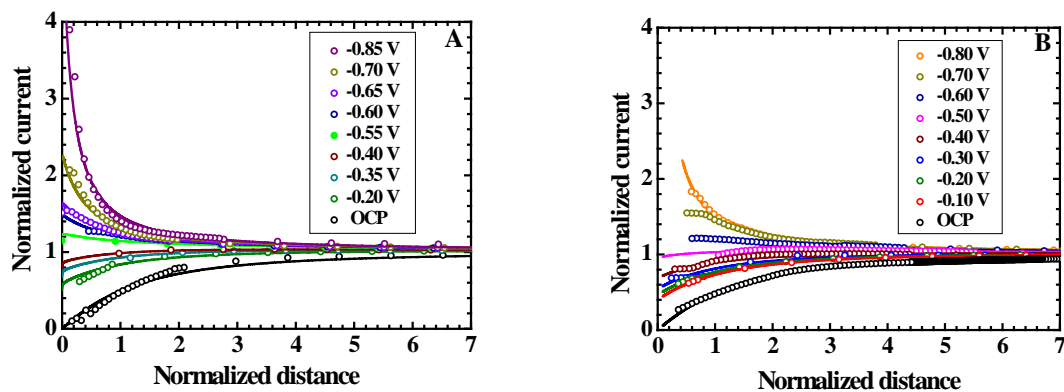
Figure 3. Comparison between experimental (symbols) and theoretical (full lines) Z-approach curves for an oxide-covered titanium sample in 0.1 M NaCl + 5 mM FcMeOH. (A) Naturally-aerated, and (B) deaerated solutions. The tip potential was set at +0.50 V vs. Ag/AgCl/(3 M) KCl, i.e, in the plateau of the ferrocene-methanol oxidation wave. Tip diameter, 25 µm; RG = 10; scan rate: 1 µm s^{-1}. Potential values of the titanium sample are referred to the Ag/AgCl/(3 M) KCl reference electrode.
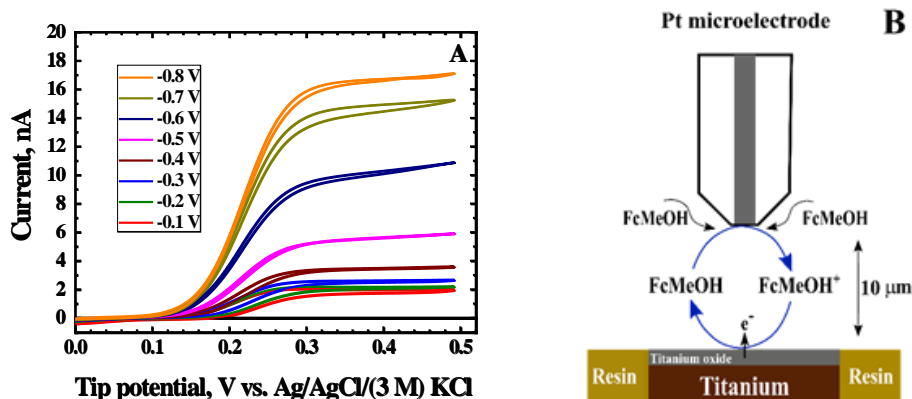
Figure 4. (A) Cyclic voltammograms recorded at the platinum tip placed over the center of an oxide-covered titanium sample at a 10 µm distance. Test solution: deaerated 0.1 M NaCl + 5 mM FcMeOH. The potential values of the titanium sample are referred to the Ag/AgCl/(3 M) KCl reference electrode. Tip diameter, 25 µm; RG = 10. Scan rate: 20 mV s^{-1}. (B) Sketch depicting a cross section of the system with indication of the positive feedback mechanism.
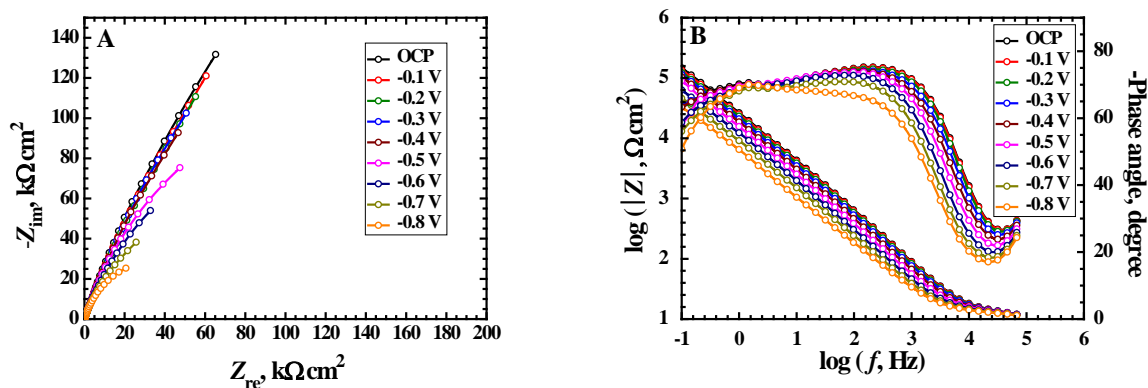
Figure 5. (A) Nyquist and (B) Bode diagrams of an oxide-covered titanium sample immersed in deaerated 0.1 M NaCl for the polarization values indicated in the graphs. Potential values indicated in the graphs are referred to the Ag/AgCl/(3 M) KCl reference electrode.
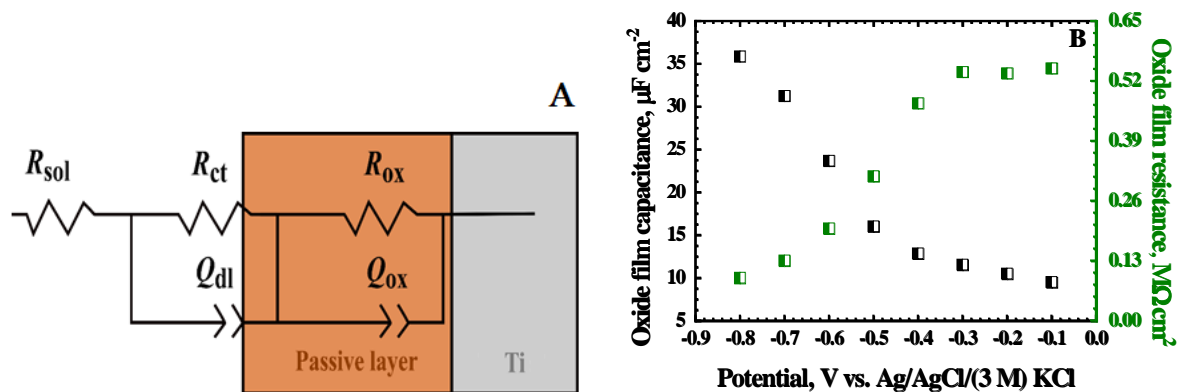
Figure 6. (A) Equivalent circuit (EC) used for the interpretation of the measured impedance spectra. (B) Effect of cathodic polarization on the resistance and the capacitance components of the oxide-covered titanium sample.
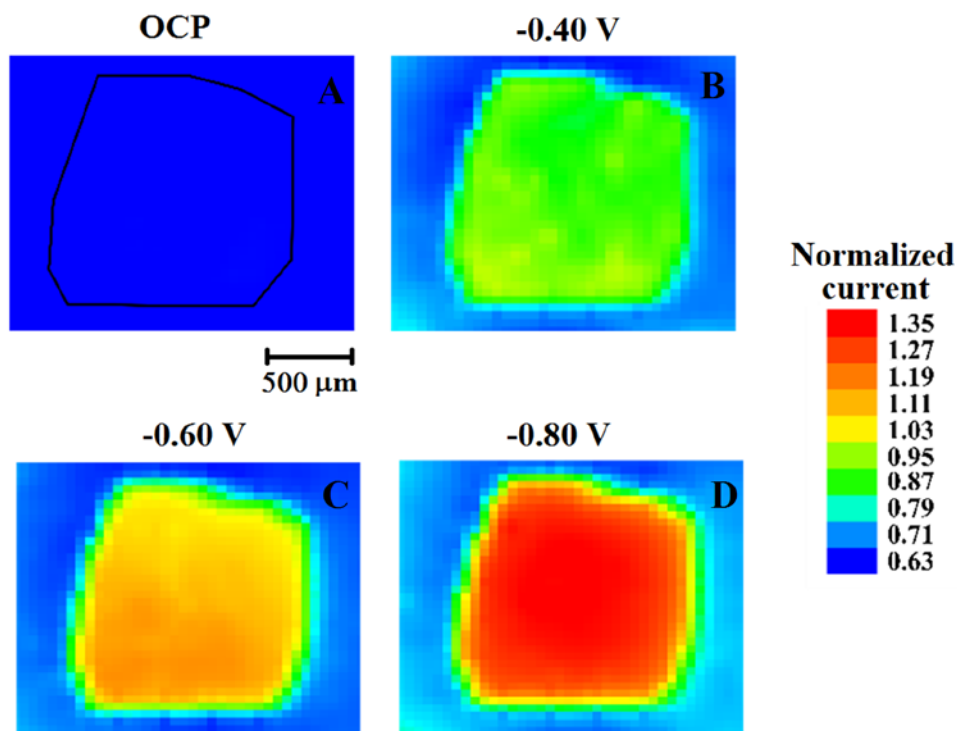

Figure 7. 2D-images generated by SECM of an oxide-covered titanium sample immersed in deaerated 0.1 M NaCl + 5 mM FcMeOH for the polarization values indicated in the graphs. Substrate potential values: (A) OCP; (B) -0.40, (C) -0.60, and (D) -0.80 V vs. Ag/AgCl/(3 M) KCl. Tip diameter, 25 µm; RG = 10; tip-sample distance, 20 µm; tip potential: +0.50 V vs. Ag/AgCl/(3 M) KCl; scan rate, 20 µm s^{-1}.
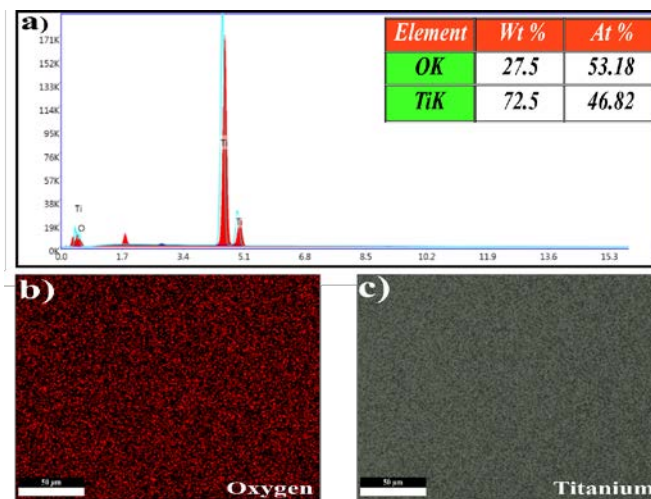
Figure 8. Elemental analysis of a titanium surface after anodic oxidation: (a) EDX spectrum; (b) and (c) elemental distribution of oxygen (Red dots) and titanium (Grey dots), respectively.
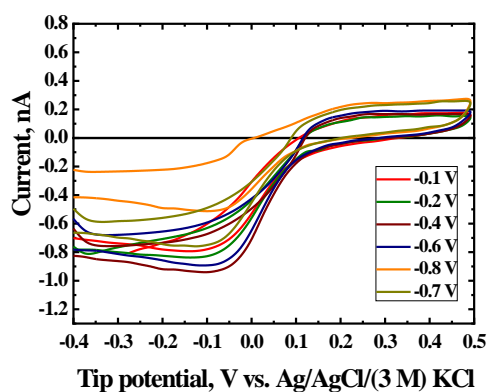

Figure 9. Cyclic voltammograms recorded at the platinum tip placed over the center of an oxide-covered titanium sample at a 10 µm distance. Test solution: deaerated 0.1 M NaCl. The potential values applied to the titanium sample are referred to the Ag/AgCl/(3 M) KCl reference electrode. Tip diameter, 25 µm; RG = 10. Scan rate: 20 mV s^{-1}.
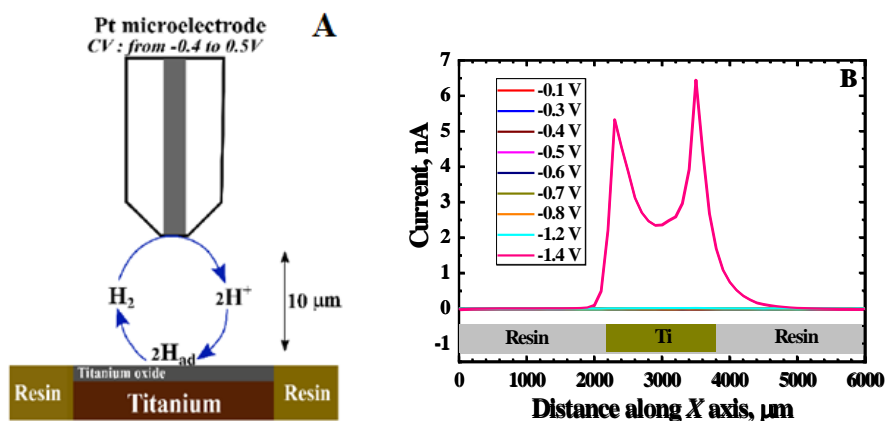

Figure 10. (A) Sketch depicting a cross section of the system with indication of the generation-collection mechanism for the monitoring of hydrogen gas evolution. (B) SECM scan lines of an oxide-covered titanium sample immersed in deaerated 0.1 M NaCl for the polarization values indicated in the graphs. Tip diameter, 25 µm; RG = 10; tip-sample distance, 20 µm; tip potential: 0 V vs. Ag/AgCl/(3 M) KCl; scan rate, 20 µm s^{-1}.
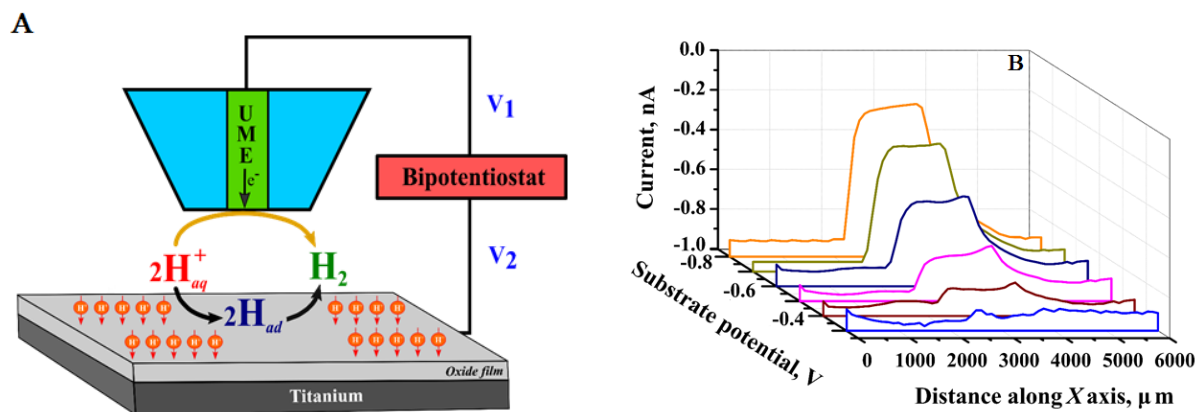
Figure 11. (A) Sketch depicting a cross section of the system with indication of the redox competition mechanism for the monitoring of hydrogen ion reduction. (B) SECM scan lines of an oxide-covered titanium sample immersed in deaerated 0.1 M NaCl for the polarization values indicated in the graph. Tip diameter, 25 µm; RG = 10; tip-sample distance, 20 µm; tip potential: -0.60 V vs. Ag/AgCl/(3 M) KCl; scan rate, 20 µm s^{-1}.